In-situ study of precipitates in Al–Zn–Mg–Cu alloys using anomalous small-angle x-ray scattering*

Chun-Ming Yang(杨春明)[1], Feng-Gang Bian(边风刚)[1,†], Bai-Qing Xiong(熊柏青)[2], Dong-Mei Liu(刘冬梅)[2], Yi-Wen Li(李怡雯)[1], Wen-Qiang Hua(滑文强)[1], and Jie Wang(王劼)[1]

[1] *Shanghai Synchrotron Radiation Facility, Shanghai Institute of Applied Physics, Chinese Academy of Sciences, Shanghai* 201204, *China*
[2] *State Key Laboratory of Nonferrous Metals and Processes, General Research Institute for Nonferrous Metals, Beijing* 100088, *China*

(Received 27 November 2015; revised manuscript received 26 February 2016; published online 20 April 2016)

In the present work, the precipitate compositions and precipitate amounts of these elements (including the size distribution, volume fraction, and inter-precipitate distance) on the Cu-containing 7000 series aluminum alloys (7150 and 7085 Al alloys), are investigated by anomalous small-angle x-ray scattering (ASAXS) at various energies. The scattering intensity of 7150 alloy with T6 aging treatment decreases as the incident x-ray energy approaches the Zn absorption edge from the lower energy side, while scattering intensity does not show a noticeable energy dependence near the Cu absorption edge. Similar results are observed in the 7085 alloy in an aging process (120 °C) by employing in-situ ASAXS measurements, indicating that the precipitate compositions should include Zn element and should not be strongly related to Cu element at the early stage after 10 min. In the aging process, the precipitate particles with an initial average size of ∼ 8 Å increase with aging time at an energy of 9.60 keV, while the increase with a slower rate is observed at an energy of 9.65 keV as near the Zn absorption edge.

Keywords: anomalous small-angle x-ray scattering, alloy, precipitates

PACS: 61.05.cf, 61.66.Dk **DOI:** 10.1088/1674-1056/25/6/066101

1. Introduction

Nanoscale precipitates of trace elements play an important role in the microstructures and performances in alloys,[1] and qualitative analyses of precipitate composition and quantitative evolution of microstructures become very necessary. Over the years, a lot of studies have focused on the nanoscale precipitates of aluminium alloys with different technologies. Transmission electron microscopy (TEM) and tomographic atom probe (TCP) can give clear information about the shapes and sizes of precipitates. However, these two methods have the disadvantages of the lower statistical analysis and inconvenience for the in-situ study in the aging process. Small-angle x-ray scattering (SAXS) enables the obtaining of many important parameters of precipitates including particle shape and length scale, so it has been widely used for characterizing the nanoscale microstructure of alloys.[2–8] When SAXS measurements are performed at different energies across the absorption edge of one of the elements present in the microstructure, we should give access to information about the composition difference between the precipitate and matrix in this specific element. Such measurements are called anomalous small-angle x-ray scattering (ASAXS), It is sensitive to the anomalous dispersion effect of a specific element.[9,10] The use of several methods could prove compositive information and complement each other.

Alloys in the Al–Zn–Mg–Cu system (7xxx series) have been extensively used as high-strength structural materials such as in the aerospace and automotive industries. The precipitate characteristics and mechanism have been investigated to probe the relationship between the precipitates and applied properties of Al alloy. TEM investigations reported that smaller clusters were found at 7050 alloy after a short aging time at 121 °C, while larger precipitates were observed with increasing aging time.[11] SAXS measurements[6,12] were carried out on the Al–Zn–Mg–Cu alloy (7150 and 7108.5) with different aging treatments, showing the evolutions of the volume fraction and particle size during aging–retrogression–reaging treatment. SAXS investigations also suggested that there are two types of particles with different sizes (smaller Guinier Preston (GP) zone and larger η' particles) in 7xxx series Al alloys aged at temperatures in a range between about 60 °C and 100 °C.[13] Positron annihilation spectroscopy investigations indicated that the Mg-vacancy, or Zn-vacancy or Zn_2-vacancy complex, has a significant effect on GP zone formation.[14,15] The three-dimensional (3D) atom probe analyzed by Sha and Cerezo[11] indicated that the precipitates of Zn are accompanied by Mg, while Mg-rich clusters were observed at the early-stage. They have also proposed that smaller clusters growing into blocky GPI zones at the earliest stages of aging (< 30 min) would be related to the more Mg elements in the clusters, while the Zn-rich is a probable reason of some

*Project supported by the National Natural Science Foundation of China (Grant Nos. 11005143, 11405259, and 51274046) and the Scientific Research Foundation for the Returned Overseas Chinese Scholars, State Education Ministry of China (Grant No. [2014]1685).

†Corresponding author. E-mail: bianfenggang@sinap.ac.cn

© 2016 Chinese Physical Society and IOP Publishing Ltd

smaller clusters becoming elongated and subsequently growing into platelet η' after 30 min. Despite the fact that there are a lot of previous studies, our understanding of precipitation is still limited, and especially the quantitative information is lacking at early-stage during the in-situ probing size, density and chemistry. In this study, we are employing ASAXS to probe the precipitates on Cu-containing 7000 series aluminum alloys (7150 and 7085Al alloys), provide more information about the precipitate compositions for the investigation of the formation mechanism.

2. Experimental section

2.1. Sample preparation

Two types of 7000 series aluminum alloys (7150 and 7085Al alloys) were used in this study. A 7150 aluminum alloy plate with compositions (mass fraction) of Zn 6.56%, Mg 2.25%, Cu 2.10%, Zr 0.12%, was prepared when the solution was heat-treated first at 470 °C for 90 min and then 480 °C for 60 min, cold water quenching, followed by the typical T6 treatment (120 °C for 24 h). A 7085 aluminum alloy plate was a hot-rolled aluminum alloy plate, with compositions (mass fraction) of Zn 7.5%, Mg 1.7%, Cu 1.4%, Zr 0.12%, and Al balance. Specimens of 7085 alloy cut from the alloy plate were treated by solution at 475 °C for 120 min, cold water quenching, followed by pre-aging at 120 °C for 12 h. Here the solution treatment was carried out in order to dissolve the second phase particles (formed during casting and/or rolling) into the solid solution adequately.

2.2. SAXS measurements

SAXS experiments were performed on the BL16B1 beamline of Shanghai Synchrotron Radiation Facility (SSRF). 2D SAXS patterns were recorded by Mar165 CCD with a pixel size of 80 μm × 80 μm. Prior to the experiments, the specimens were mechanically polished into foils of about 100 μm in thickness. A sample-to-detector distance of ∼2 m was chosen, giving access to a range of scattering vector Q [0.15 nm^{-1} ∼ 3 nm^{-1}]. During the experiments, the beam size was 2 mm × 1 mm. The temperatures of the specimens were monitored by using a Linkam thermal stage THMS600 (Linkam Scientific Instruments). In-situ SAXS measurements on 7085 alloy were carried out during aging at a temperature of 120 °C. During the whole heat treatment, the temperature uncertainty is within ±0.2 °C. In the present work, one-dimensional integrated intensity curves were obtained from 2D SAXS patterns by employing Fit2D software, while SAXS data quantitative data analyses were conducted using the Irena curve fitting package within IGOR Pro.[16] In the model, a form factor of spheroid and a structure factor of a type of precipitate were chosen, and a logarithmic normal size distribution was used to account for the polydispersity. The mean radius, distance, size distribution of precipitates, etc. would be obtained.

3. Results and discussion

3.1. ASAXS investigation of precipitate compositions

Figure 1 shows I versus q plots for different energies of the x-ray beam at the two absorption edges, in the case of the 7150 alloy after aging treatment of T6. In Fig. 1(a), the SAXS intensity is found to apparently decrease as the incident x-ray energy approaches the absorption edge of Zn from the lower energy side. In contrast, as shown in Fig. 1(b), the SAXS intensity decreases very slightly only when the energy is close to the absorption edge of Cu. The results clearly indicate that the copper should not play a significant role in the intensity of the small angle region due to its uniform distribution, while the measured SAXS intensity should be related to fluctuation in the electron density of zinc in 7150 alloy. Similar results also are observed in 7050 alloy during aging at 121 °C,[11] in which 3DAP method shows that the GP zones include mainly Zn and Mg atoms, while the Cu should have a small amount of content in the precipitates. It is interesting to note that the peaks in all SAXS profiles in Figs. 1(a) and 1(b) are almost all at a value of ∼ 0.64 nm^{-1}, which should correspond to a spatial length scale of the gyration radius R_g (∼ 2 nm) obtained

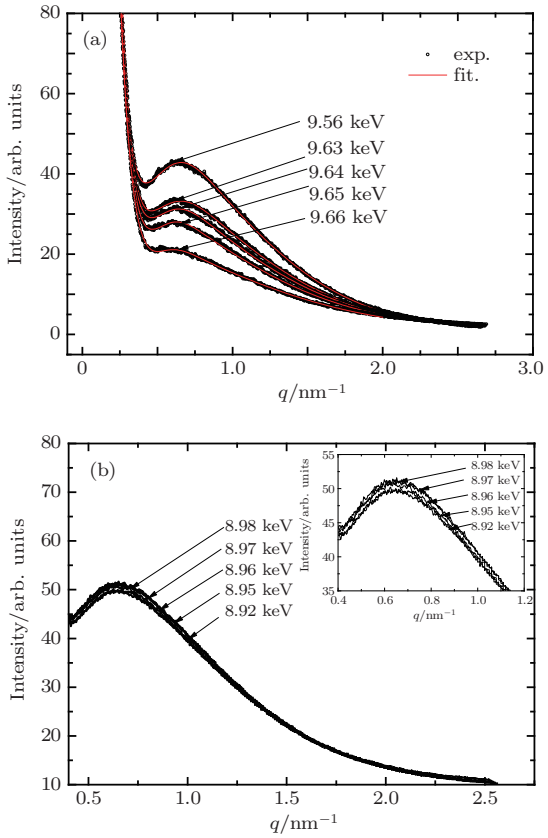


Fig. 1. (color online) Scattered intensities of 7150 alloy after T6 treatment obtained at various energies: below the Zn absorption edge (a) and close to the Cu absorption edge (b). The inset in panel (b) shows the enlarged low-q parts of selected SAXS profiles. The solid lines represent the results fitting to the experimental data.

by employing a relationship $q_{\max} = 3^{1/2}/R_g$. The micrographs of bright-field (BF) TEM for 7150 alloy after T6 treatment support such a length scale for the precipitates as shown in Fig. 2.

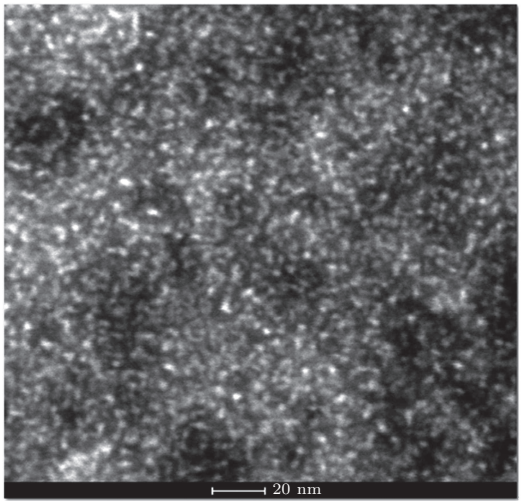


Fig. 2. Bright-field TEM micrographs for 7150 alloy after T6 treatment.

In each SAXS profile of Fig. 1(a), the fitted curves are denoted with the red solid lines. The structural parameters are obtained from fitting at various energies below the Zn absorption edge as listed in Table 1. It is seen that the mean radius of precipitate clusters increases with the decrease of energy as it is close to the Zn absorption edge; while the inter-precipitate distance decreases. It indicates that the Zn element should be contained in the precipitate particles, and these particles would be other elements. It is also suggested that Zn element is mostly scattered in the precipitate clusters, in other words, the precipitate cluster cannot be modeled as a typical shell. The calculated volume fractions of the precipitates in the 7150 Al alloys are in a range of $2\% \sim 3\%$, similar to that reported in Ref. [5]. Figure 3 shows the calculated distributions of volume fractions each as a function of precipitate size, obtained at various energies. The peak values shift with energy decreasing from 1.4 nm obtained at energy of 9.56 keV to 0.9 nm at 9.66 keV. The precipitate sizes range from 0.5 nm to 2.5 nm, which are consistent with the TEM results shown in Fig. 2.

Table 1. Structural parameters obtained from fitting for 7150 Al alloy after T6 treatment, obtained at various energies below the Zn absorption edge.

	9.56/keV	9.63/keV	9.64/keV	9.65/keV	9.66keV
Mean radius/nm	1.44	1.33	1.29	1.23	1.16
Inter-precipitate distance/nm	5.31	5.26	5.56	5.80	6.84
Volume fraction/%	2.83	2.51	2.48	2.32	2.12

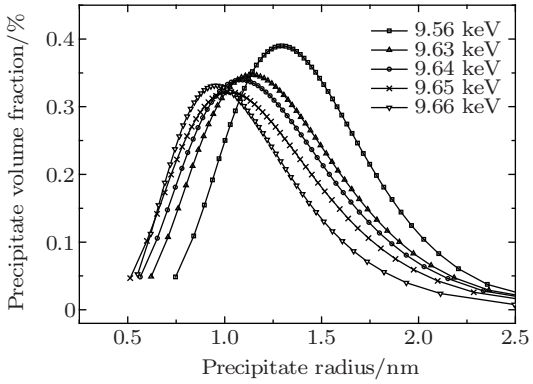


Fig. 3. Distributions of volume fraction obtained at various energies as a function of precipitate size for the 7150 alloy after T6 treatment.

3.2. *In-situ* ASAXS investigation of precipitates

Figure 4 shows SAXS profiles at selected energies below Zn absorption edge for the 7085 alloy during aging at 120 °C. At an earlier stage such as at 50 min (Fig. 4(a)), the SAXS profile obtained at an energy of 9.63 keV overlaps with the profile obtained at an energy of 9.65 keV. With increasing aging time (Figs. 4(b) and 4(c)), the scattering intensity in a lower q region (0.3 nm^{-1}–1.8 nm^{-1}), obtained at 9.63 keV, increases and the two profiles gradually approach the separated condition. The results clearly show that the precipitate particles could contain Zn element.

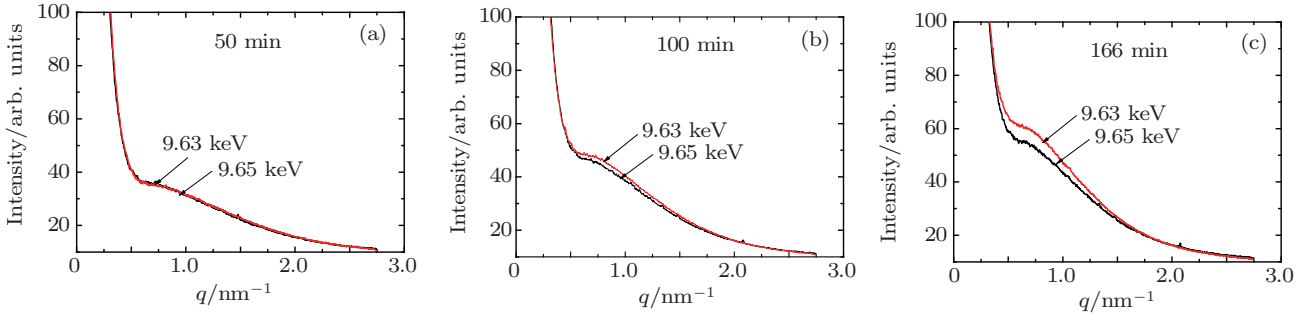


Fig. 4. (color online) SAXS profiles obtained at different energies (9.63 keV and 9.65 keV) and different stages (50 min (a), 100 min (b), and 166 min (c)) for the 7085 alloy during aging at 120 °C.

Figure 5 shows SAXS profiles obtained during aging at a temperature of 120 °C for 7085 alloy. The incident energy of 9.60 keV is below Zn absorption edge. With increasing aging time, the scattering intensity distinctly increases in a lower q region. It is clearly indicated that the alloy has precipitation during aging at a temperature of 120 °C. Figure 6 shows the calculated distributions of volume fractions each as a function of precipitate size, for the alloy aged at various times. The striking feature is that the standard deviation of the precipitate size distribution is observed to gradually increase with aging time increasing. It is initially contracted, and increases by a factor of two during the aging. This feature could be explained as the fact that the growth of stable particles is somewhat compensated for by the presence of small particles, because some small particles dissolving can result in a constant average radius of the precipitate size distribution. The precipitate size (radius) ranges from 0.6 nm to 2.6 nm, which is consistent with TEM result of 7085 alloy obtained after the aging of 233 min (the inset of Fig. 6).

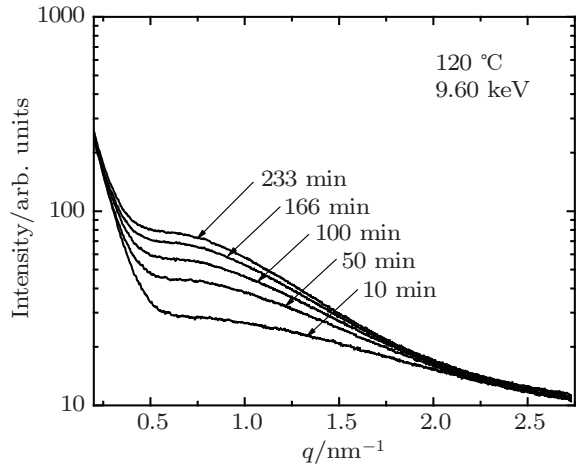


Fig. 5. SAXS profiles obtained during aging at a temperature of 120 °C for 7085 alloy. The incident energy of 9.60 keV is below Zn absorption edge.

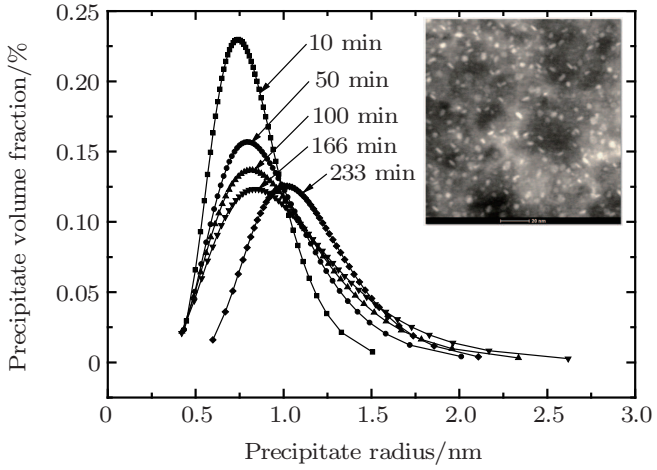


Fig. 6. Variations of distribution of volume fraction with precipitate size for the 7085 alloy during aging at 120 °C. The inset shows bright-field TEM micrograph for 7085 alloy after aging.

In Fig. 7, the variations of the mean radius of precipitate clusters with aging time obtained at energy of 9.65 keV (solid circles) and 9.60 keV (solid squares) respectively. For energy very near the Zn absorption edge, the growth rate of precipitate clusters is slower than that at an energy of 9.60 keV, suggesting that the precipitate clusters not only contain Zn element, but also are zinc-rich. A usual precipitation sequence of Al alloys (7xxx series) should include the following processes:[17] 1) solid solution; 2) GP zones (GPZs); 3) metastable η'; 4) stable ($MgZn_2$). GPZs (GPI and GPII) and η' often form during the early stages of precipitation (from quench for up to 1 day). The three-dimensional atom probe (3DAP) measurements[11] suggest that the smaller clusters (Mg-rich) should grow into blocky GPI at the earliest stages of aging (the first 30 min aging), while the more Zn-rich small clusters after 30 min aging would become elongated and subsequently grow into platelet η'. The present ASAXS result as shown in Fig. 4 indicates that the Zn-rich clusters are grown up after about 50 min aging at 120 °C, which is consistent with results in Ref. [11].

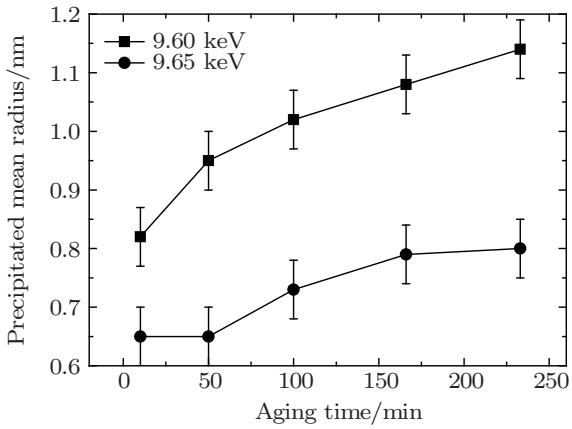


Fig. 7. Variations of precipitate mean radius with aging time, obtained at energies of 9.65 keV (solid circles) and 9.60 keV (solid squares), respectively.

4. Conclusions

We investigate Al alloys of 7150 and 7085 at energies near the Zn and Cu absorption edge using ASAXS. We find that scattering intensity decreases as the incident x-ray energy approaches the Zn absorption edge from the lower energy side, while the scattering intensity does not show a noticeable energy dependence near the Cu absorption edge. The in-situ ASAXS probing during aging at 120 °C, shows that the SAXS profile obtained near the Zn absorption can be distinguished after 50-min aging, which indicates that the more Zn-rich smaller clusters could be elongated and subsequently grow into platelet η' after 50 min.

References

[1] Ringer S P and Hono K 2000 *Mater. Charact.* **44** 101

[2] Deschamps A, Lae L and Guyot P 2007 *Acta Mater.* **55** 2775
[3] Marlaud T, Deschamps A, Bley F, Lefebvre W and Baroux B 2010 *Acta Mater.* **58** 4814
[4] Yu C F, Koh S, Leisch J E, Toney M F and Strasser P 2008 *Faraday Discuss.* **140** 283
[5] Liu D M, Xiong B Q, Bian F G, Li Z H, Li X W, Zhang Y A, Wang F and Liu H W 2013 *Mater. Sci. Eng. A* **588** 1
[6] Liu D M, Xiong B Q, Bian F G, Li Z H, Li X W, Zhang Y A, Wang F and Liu H W 2014 *Mater. Des.* **56** 1020
[7] Sun G A, Chen B, Wu E D, Yan G Y, Huang C Q, Li W H, Wu Z H, Liu Y and Wang J 2011 *Acta Phys. Sin.* **60** 016102 (in Chinese)
[8] Li X Y, Li X H, Yang C H, Hua W Q, Zhao N, Miao X R, Tian F, Wang Y Z, Bian F G and Wang J 2013 *Chin. Phys. B* **22** 046102
[9] Waseda Y 2002 *Anomalous X-ray Scattering for Materials Characterization* (New York: Springer)
[10] Marlaud T, Deschamps A, Bley F and Baroux B 2008 11*th International Conference on Aluminium Alloys* (ICAA11) **1** 954, Aachen, Germany
[11] Sha G and Cerezo A 2004 *Acta Mater.* **52** 4503
[12] Nicolas M and Deschamps A 2003 *Acta Mater.* **51** 6077
[13] Groma G, Kovacs-Csetenyi E, Kovas I, Lendvai J and Ungar T 1979 *Phil. Mag. A* **40** 653
[14] Dlubek G, Krause R, Brümmer O and Plazaola F 1986 *J. Mater. Sci.* **21** 853
[15] Ferragut R, Somoza A and Dupasquier A 1998 *J. Phys.: Condens. Matter* **10** 3903
[16] Ilavsky J and Jemian P R 2009 *J. Appl. Cryst.* **42** 347
[17] Degischer H P, Lacom W, Zahra A and Zahra C Y 1980 *Z. Metallk.* **71** 231